Calcif Tissue Int (1984) 36:596–603

Calcified Tissue International

Calcium Distribution In Freeze-Dried Enamel Organ Tissue During Normal and Altered Enamel Mineralization

D. R. Eisenmann, S. H. Ashrafi, and A. E. Zaki

Department of Histology, University of Illinois, Box 6998, Chicago, Illinois 60680

Summary. Energy dispersive X-ray microanalysis was applied to freeze-dried blocks of enamel organ tissue to determine levels of calcium in various cellular regions. The tissue blocks were dissected free from adjacent forming enamel following injection of cobalt or fluoride ions, both of which temporarily inhibit enamel mineralization. In all control and experimental specimens there was an increasing gradient of calcium from the stratum intermedium cells to the distal ends of the ameloblasts. Calcium levels were significantly reduced near the distal ends of the ameloblasts following cobalt or fluoride injection as compared with controls. It is suggested that evidence of an intercellular buildup of calcium near the distal ends of the ameloblast supports a controlling function of these cells. The changes in calcium levels are correlated with alterations in mineralization known to occur in the adjacent enamel of the model systems employed.

Key words: Calcium — Ameloblasts — X-ray microanalysis — Transport — Frozen.

It has been established that calcium traverses enamel organ cells to reach the mineralizing enamel rather than entering from the pulpo-dentinal side [1, 2]. The distribution of calcium in relation to enamel-forming cells and their role in controlling calcium transport are unclear. Calcium has been localized autoradiographically and cytochemically both within and between the ameloblasts in chemically preserved tissues [3, 4]. One group of investigators using X-ray microanalysis of freeze-dried tissue found uniformly low calcium levels over secretory ameloblasts [5, 6], but another reported substantially higher concentrations under similar conditions [7]. There is very little direct evidence linking cell-related calcium in enamel-forming tissues with the mineralizing process.

A model system has been developed in which enamel mineralization in the rat incisor is temporarily inhibited by injection of substances such as sodium fluoride and cobalt chloride [8, 9]. This sytem provides opportunity to assess the calcium concentration of enamel organ tissue during a temporary interruption of enamel mineralization. Initial cytochemical investigation has revealed some shifts in the intracellular distribution of calcium during the period of disturbance in mineralization [9].

Most previous analytical investigations employed chemical fixation of tissue which may cause dislocation of calcium and thin sections that contain too little of the ion for detection by routine energy dispersive X-ray microanalysis. The purpose of this study is to apply X-ray microanalysis to compare the concentrations of calcium in various regions of anhydrously preserved enamel organ tissue during normal and altered enamel formation.

Materials and Methods

Male rats weighing 150–200 g were divided into three groups, each of which consisted of three animals. The first group received injections of sodium fluoride (5 mg/100 g body weight) and were killed by ether overdose one hour later. The second group received injections of cobalt chloride (12 mg/100 g) and the same subsequent treatment. The third group (controls) received no injection but were otherwise handled in the same manner as the experimental groups. Upper incisors and their adherent alveolar bone were dissected quickly from surrounding tissues. One incisor was partially dislocated from its socket by manual pressure which caused a separation of 1–2 mm to occur between the distal ends of the ameloblasts and the forming enamel surface. This procedure was completed within approximately one minute after death of the animal, and the incisor was then immediately frozen for 15 sec in isopentane, (−150°C) chilled with liquid nitrogen.

Send reprint requests to Dr. D. R. Eisenmann at the above address.

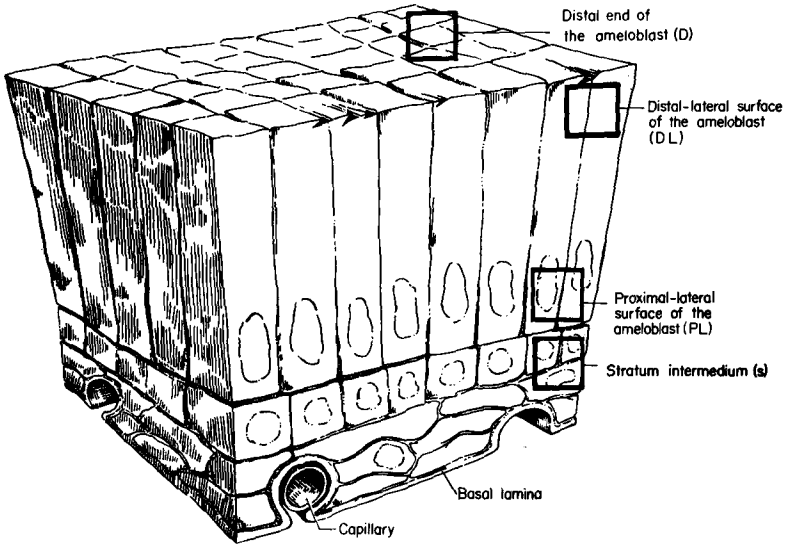

Fig. 1. Diagram of a block of freeze-dried enamel organ tissue, × 1,000. Three of the analytical regions are indicated on the lateral fractured surface of the tissue and the fourth (distal end of the ameloblast) is on the distal surface which had been separated from the adjacent enamel.

The contralateral incisor was processed in one of two different manners for transmission electron microscopy. In the first instance, separated enamel organs were placed in 2% glutaraldehyde buffered with .05 M potassium acetate for determination of the location where separation had occurred. In the second instance, the whole incisor (without fracturing) was sectioned longitudinally by a previously described method [10] and immersed in acetate-buffered glutaraldehyde fixative to document the inhibition of mineralization induced by cobalt and fluoride. In both instances these specimens were postfixed in 1% osmium tetraoxide and processed routinely for examination by transmission electron microscopy.

The specimens that had been chilled in isopentane were transferred into liquid nitrogen and freeze-dried at −35°C in a cryostat under vacuum for two days. After drying, the enamel organ was separated from adjacent tissues using micro-dissection techniques. To be certain that enamel organ tissue in the secretory zone was used, measurements were made from the growing tip based on information derived from longitudinal sections of comparable rat incisors. The freeze-dried enamel organs were then fractured in a plane parallel to the long axis of the tooth. This exposed the lateral surface of the ameloblasts and the adjacent stratum intermedium cells. This lateral surface as well as the distal ends of the separated ameloblasts were later used for microanalysis (Fig. 1).

The freeze-dried specimens were mounted on carbon studs and coated with evaporated carbon at a thickness of 400 A. They were examined in a scanning electron microscope attached to an energy-dispersive X-ray analyzer system. The X-ray analyzer was connected to an 8 K memory-size computer programmed with EM software supplied by the manufacturer of the analyzer. Spectra were recorded in the range of 0.0–8,000 eV with 20 eV per channel. The operating condition of the analyzer was 100 s for recording spectra at 20 kV and a beam current of 160 μA. The tilt angle was 45° and take-off angle 30°. The beam size was around 1,000 A. The calcium peak was recorded at 3,700 eV. The element counts per 100 sec were determined by using a computer program which subtracted background and corrected for overlapping of elemental peaks by documented methods [11–13]. A minimum of 12 readings was recorded for each region analysed. Figure 1 illustrates the four regions selected for microanalysis: stratum intermedium cells, proximal and distal areas of the lateral fractured surface of the secretory ameloblasts, and the distal ends of the ameloblasts. Both cellular and intercellular regions were included in each analysis. The analytical volume consisted of a surface area of 8 × 8 μm and an estimated depth of 7–15 μm.

Results

Transmission electron micrographs of thin sections from the chemically fixed tissues were examined to be certain that only soft tissues were included in the enamel organ specimens. Figure 2 illustrates secretory ameloblasts which had been manually separated from the adjacent enamel. Although the method of fixation utilized for these specimens did not provide good preservation of cellular detail, it was possible to ascertain that the separation occurred in the region of the distal intercellular junctions, leaving all mineralized enamel and Tomes' processes behind on the tooth surface. It was also confirmed that the experimental animals were responding as expected to either cobalt or fluoride by accumulating stippled material at the mineralization front (Fig. 3).

The freeze-dried specimens used for microanalysis presented a large rather flat distal surface (formerly in contact with enamel), and perpendicular to it a fractured lateral surface which runs parallel to the long axis of the ameloblasts (Fig. 4A). Individual secretory ameloblasts and adjacent stratum intermedium cells could be readily distinguished on the lateral fractured surface (Fig. 4B). Higher magnification scanning electron micrographs of the distal surfaces revealed distortion caused by ice crystal formation during the freeze-drying process. However, the rough outline of individual cells could

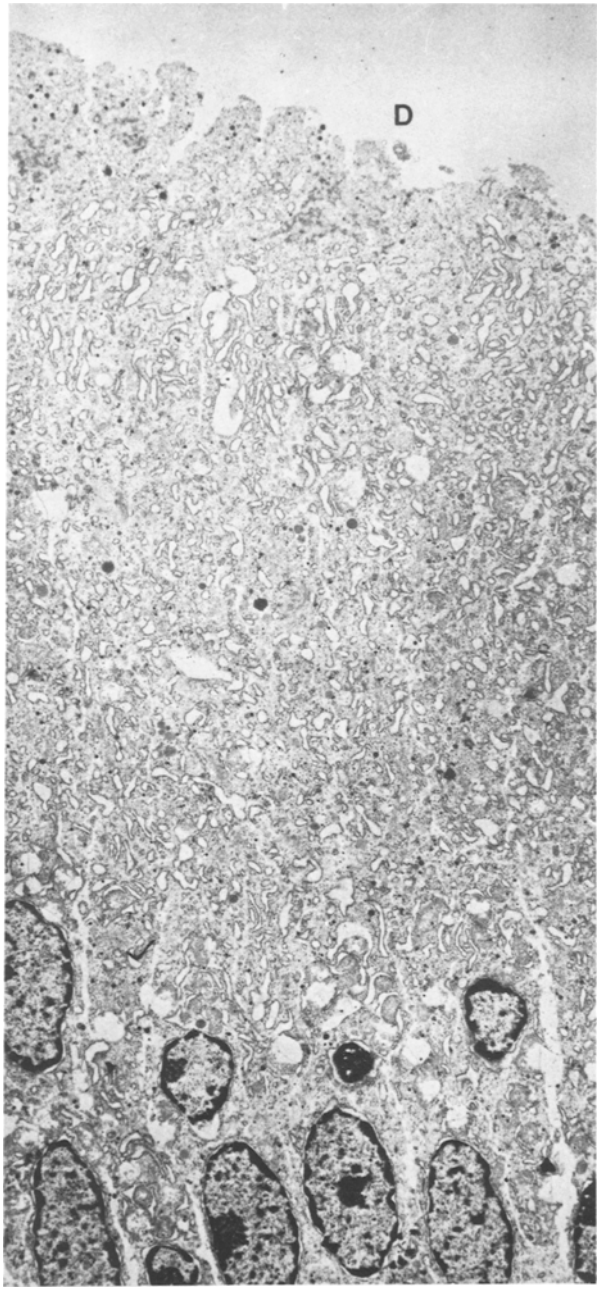

Fig. 2. Transmission electron micrograph of secretory ameloblasts in enamel organ tissue handled in the same manner as the freeze-dried specimens but fixed instead in glutaraldehyde, × 3,800. *D*-distal end of ameloblasts.

be discerned. The morphology of the distal ends of control and fluoride-injected specimens (Fig. 4C) consisted of distinct peaks of cellular material rising from rather thin plates of tissue. Cobalt injected specimens (Fig. 4D) displayed more flattened distal ends with thicker plates of cellular material forming a smooth network.

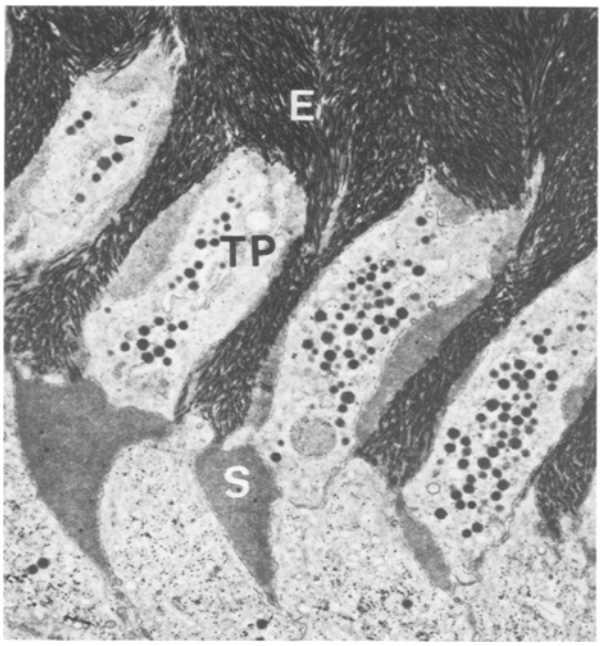

Fig. 3. Transmission electron micrograph of Tomes' process (*TP*) region of fixed secretory ameloblasts from rat injected with cobalt chloride, × 8,600. *S*-stippled material, *E*-mineralized enamel.

Spectra of X-ray microanalyses included peaks for calcium, phosphorous, sulfur, chlorine, and potassium. Representative spectra with and without background from the distal ends as well as the lateral surfaces of ameloblasts are illustrated in Fig. 5. Calcium peaks were always highest in analyses taken from the distal ends of the ameloblasts.

Table 1 lists the means of element counts /100 sec for calcium in the four regions analysed for all specimens. In every animal (control and experimental) there was a progressive increase in calcium levels starting at the stratum intermedium cells and concluding with the distal ends of the ameloblasts. This table also contains means for each animal group for the four regions analysed. A marked reduction in calcium levels occurred in response to both fluoride and cobalt as compared with controls. This reduction was statistically significant for the two sets of analyses taken near the distal ends of the ameloblasts, and the trend was in the same direction in the more proximal areas as well. The greatest reduction in calcium levels occurred in the cobalt specimens.

Figure 6 is a histogram of the data by animal groups for the four regions analysed which clearly illustrates the similar trends among the groups. Although the fluoride and cobalt specimens experienced significant reductions in calcium levels at their ends, the pattern of increasingly higher levels

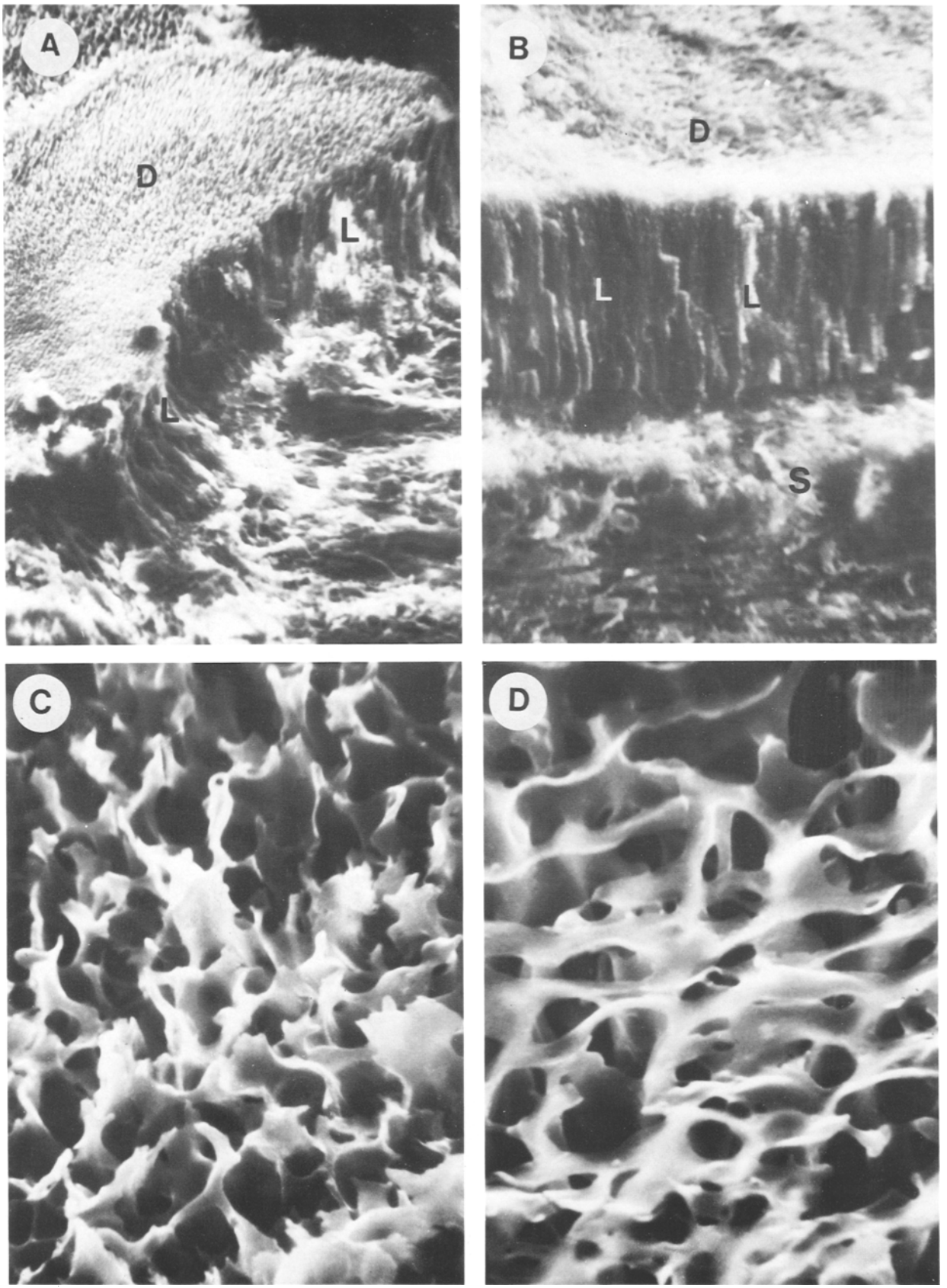

Fig. 4. Scanning electron micrographs of freeze-dried enamel organ tissue used for elemental analysis. **A.** Low power view of block of tissue fractured in a line parallel to the longitudinal axis of the ameloblasts, ×250. *D*-distal end of ameloblasts, *L*-lateral (fractured) surface of ameloblasts. **B.** Medium power view of enamel organ illustrating individual secretory ameloblasts, ×500. *D*-distal ends of ameloblasts, *L*-lateral (fractured) surface of ameloblasts, *S*-stratum intermedium cells. **C.** High magnification of distal ends of control secretory ameloblasts, ×2,500. **D.** High magnification of distal ends of secretory ameloblasts from rat injected with cobalt chloride, ×2,500. Note difference in morphology of the fractured ends of these ameloblasts as compared with controls.

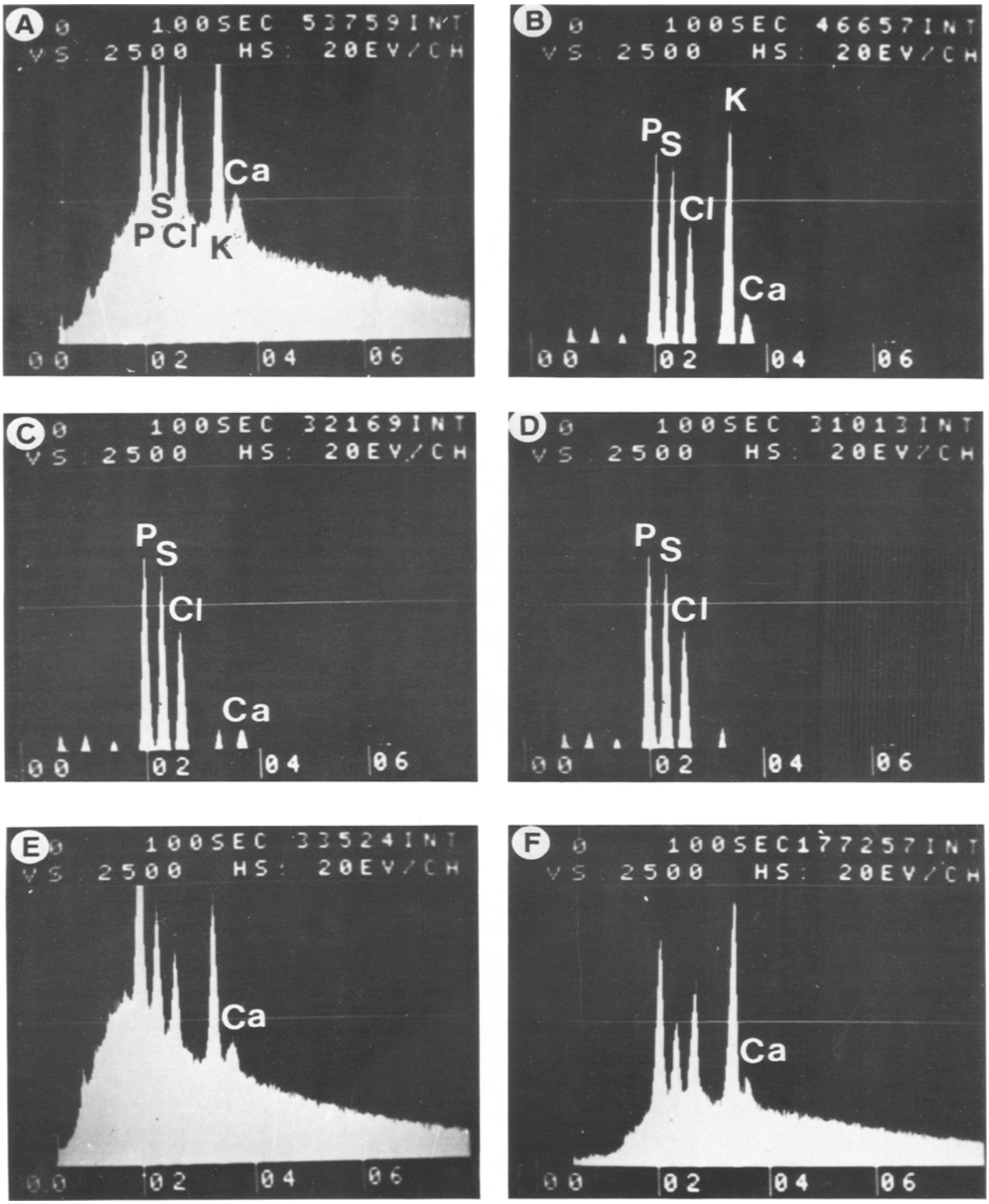

Fig. 5. Energy dispersive X-ray microanalysis spectra of the distal ends of the ameloblasts, **(A–D),** the distal lateral surface of the ameloblasts **(E)** and the proximal lateral surface of the ameloblasts **(F). A.** Spectrum showing clearly identifiable peaks for phosphorus (*P*), sulfur (*S*), chloride (*C*1), potassium (*K*) and calcium (*Ca*) (Region D in Fig. 1). **B.** The background was stripped from the spectrum illustrated in 5A. Note the prominent X-ray signal for *K* and a significantly lower one for *Ca*. **C.** The same spectrum as 5A except that the potassium Kα and Kβ peaks were stripped. The calcium Kα signal remains indicating that the peak is that of calcium and is not a potassium Kβ peak. **D.** In this spectrum (same as 5A) the EDIT aided computer system was applied for stripping calcium signals. Note the lack of a calcium Kα peak, further evidence that the Ca peaks observed in Figs. A–C are due to calcium X-ray signals and not to an overlapping peak from another element. **E.** Spectrum of the distal lateral surface of the ameloblasts (Region *DL* in Fig. 1). The reduction in height of the calcium peak as compared with that shown in Fig. 5A indicates a relatively lower calcium concentration. **F.** Spectrum of the proximal lateral surface of the ameloblasts (Region *DL* in Fig. 1). Note the weak calcium X-ray signals as compared with those in Figs. 5A and 5E, indicating lower calcium concentration in *PL* than in *DL* and D regions.

Table 1. Mean calcium counts/100 sec for each specimen[a] and combined means for each animal group by region of analysis

	Stratum intermedium cells		Proximal lateral ameloblasts		Distal lateral ameloblasts		Distal ends ameloblasts	
	Mean	±SEM	Mean	±SEM	Mean	±SEM	Mean	±SEM
Control group								
1	313	± 27	581	± 80	775	± 51	1013	± 120
2	308	± 39	589	± 38	742	± 40	1009	± 113
3	262	± 59	334	± 40	589	± 32	1075	± 221
Group								
mean ± SEM	*294*	± 16	*501*	± 84	*702*	± 57	*1032*	± 21
Fluoride-injected								
1	230	± 33	349	± 30	398	± 57	629	± 86
2	241	± 31	358	± 45	457	± 45	811	± 38
3	260	± 29	337	± 53	368	± 33	585	± 73
Group								
mean ± SEM	*244*	± 8	*348*	± 6	*408*[c]	± 26	*675*	± 69
Cobalt-injected								
1	192	± 21	269	± 90	305	± 21	609	± 123
2	197	± 36	271	± 31	366	± 72	513	± 49
3	307	± 50	372	± 42	439	± 90	532	± 33
Group								
mean ± SEM	*232*	± 38	*304*	± 34	*370*[c]	± 39	*551*[b]	± 29

Student *t* test was used to measure statistical significance between group means of control animals vs fluoride-injected and cobalt-injected ones

[a] Minimum of 12 readings for each region

[b] Significantly different from control group mean at $P < .001$

[c] Significantly different from control group mean at $P < .01$

from proximal to distal was still present although less striking than in the controls.

Discussion

X-ray microanalysis of anhydrously preserved enamel organ tissue has demonstrated reductions in calcium levels in this tissue which correspond with inhibition of mineralization of adjacent enamel. Freeze-dried secretory ameloblasts were similar in morphologic appearance to those observed by others using SEM to examine critical point-dried rat incisors fractured in the same plane [14, 15]. The mechanically separated enamel organs consisted of soft tissue only. TEM examination confirmed that separation had occurred just proximal to the distal junctional complex with the bulk of the ameloblasts remaining intact. The brief time period between death of the animal and freezing is comparable to that which occurs when such tissues are preserved by immersion fixation. It is unlikely that any significant diffusion of calcium into the ameloblasts from the enamel surface could occur since most of the calcium is in a precipitated form in the newly secreted enamel. In addition, the most distal portions of these cells (Tomes' processes), which are

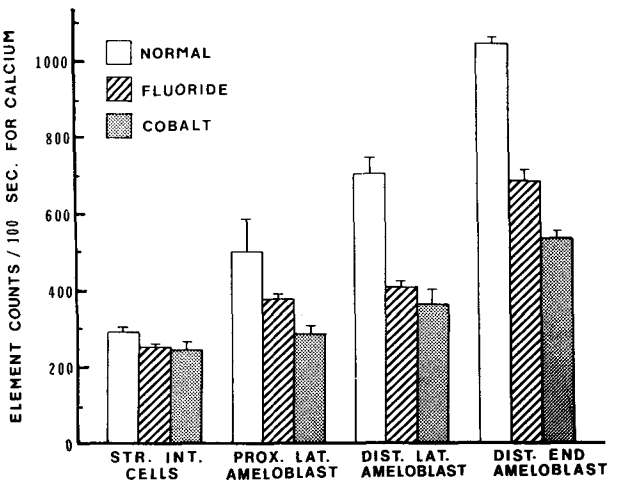

Fig. 6. Histogram of element counts/100 sec for calcium in four analytical regions. Calcium concentration is reduced by fluoride and cobalt injection and most noticeably near the distal ends of the secretory ameloblasts.

in contact with the enamel surface, remain with the enamel following separation.

A typical inhibitory response was produced by the fluoride and cobalt injections. As observed in previous studies [8, 9], mineralization was interrupted and substantial amounts of stippled material

were being released at the secretory regions of Tomes' processes. It has been demonstrated that these large accumulations of stippled material are a response to the injected ions and not a result of postmortum changes due to the method of fixation employed (Chen and Eisenmann, in preparation).

The progressively higher levels of calcium from proximal to distal regions most likely represent a concentration of extracellular and/or membrane associated calcium in the region of the distal intercellular junctions. This interpretation is based upon several previously reported observations and hypotheses. *In vitro* studies have demonstrated that viable enamel organ cells slow the movement of calcium from the exterior to the enamel surface [16]. It has also been reported that although the proximal junctional complexes of the secretory ameloblast provide an incomplete seal, the distal junctional complexes offer progressively greater resistance to penetration as enamel formation proceeds [17, 18]. Previous cytochemical and autoradiographic investigations have shown much larger concentrations of calcium between the cells (or along their membranes) than within them [3, 4]. In addition, it is well known that physiologic levels of extracellular calcium are generally three levels of magnitude higher than cellular levels [19, 20]. It has been proposed that an intercellular pathway is traversed initially by calcium and that it then enters the secretory ameloblast at the region of the distal intercellular junctions [21]. It has also been suggested that calcium may travel within the substance of the ameloblast cell membrane by carrier all the way to the enamel front where it is released [22]. Whatever regulating or concentrating mechanisms may be involved, it is clear that further attention should be focused upon the activities of calcium in relation to cytologic elements located near the distal end of the secretory ameloblast.

It is also possible that the normal accumulation of secretory granules near the distal end of the ameloblast may contribute somewhat to the higher concentration of calcium in this region. Our previous studies using potassium pyroantimonate cytochemistry [9] and electron energy loss spectroscopy (Zaki, Eisenmann, Ashrafi, Leapman and DiFiori, in preparation) revealed the presence of calcium in these granules.

In our cytochemical investigation, no changes in intercellular calcium were observed following fluoride injection [9]. However, those tissues were preserved by chemical fixation which is believed to retain less of the total calcium than anhydrous methods of preparation. In the same study, we applied the X-ray microanalysis method to enamel organ tissue fixed with glutaraldehyde and found that the calcium levels in fluoride-injected animals differed little from the controls. The marked difference in results in the present study using anhydrous preservation indicates that some of the calcium destined for mineralization is of a loosely bound form, a portion of which can be readily lost during chemical fixation.

During the secretory stage of amelogenesis, mineralization is occurring both at the developing surface in the form of initiation of new crystals and in deeper layers by growth of older crystals. Previous studies of the inhibitory effects on mineralization of fluoride and cobalt indicate differences in responses to these ions [8]. During the active fluoride response there is an inhibition of formation of new crystals whereas preinjection enamel continues to accumulate mineral. The response to cobalt is more extensive in that both new crystal formation and increased mineral density of deeper layers are inhibited. This corresponds with our current observation that cobalt caused a greater decrease in enamel organ calcium than fluoride. It appears that crystal growth in deeper layers continues in the presence of moderately reduced levels of calcium in enamel organ tissue (fluoride response) but that it is inhibited when there is a greater reduction in calcium (cobalt response). The more severe response to cobalt injection may also be reflected in the altered morphological appearance of the distal separated ends of these ameloblasts.

Mechanisms controlling calcium availability for the initiation of new crystals may be different from those involved in growth of older crystals. It is well known that crystal growth can occur primarily as a physicochemical phenomenon, whereas there is increasing evidence to support cellular control of new crystal formation [23]. Our cytochemical studies have demonstrated a reduction in calcium associated with secretory granules in response to both cobalt and fluoride [9, 24]. We have proposed that this calcium may serve as a crystal seeding component in the organic matrix after its secretion. It appears that whatever mechanisms are responsible for initiation of new crystals, this activity may be more sensitive to changes in enamel organ calcium levels than is growth of existing crystals. In a previous clinical survey of various forms of enamel hypoplasia, it was observed that systemic hypocalcemia was a common feature [25]. It was speculated that enamel defects in fluorosis and strontium rickets might result rather from a localized diminution in calcium activity in the environment of the ameloblasts where these ions are concentrated. Our data provide evidence for this proposed localized decrease in calcium concentration.

The results of this study indicate that the con-

centration of calcium near the distal end of the secretory ameloblast may be an important factor in normal enamel mineralization. This concentration of calcium is probably dependent upon enzyme activity, controlled ion transfer across cell junctions, and special characteristics of carrier molecules. Whether or not a significant amount of calcium passes through the cell itself remains unclear. In either case it appears that the region of the distal junctional complex exerts regulating influence. This study provides additional evidence to support an important role for the ameloblast in controlling calcium availability for mineralization.

Acknowledgments. We wish to acknowledge the technical assistance of Isabel and Loretta Stoncius, Elena Baltrusaitis, Eugenia Kraucunas, and Daniel Gandor. We are indebted to Elizabeth Fink for the schematic diagram. This study was supported in part by PHS Grant DE05323.

References

1. Reith EJ, Cotty VE (1962) Autoradiographic studies on calcification of enamel. Arch Oral Biol. 7:365–372
2. Wennberg A, Bawden JW (1978) Influence of the pulpal route on uptake of ^{45}Ca in enamel and dentin of developing rat molars. J Dent Res 57:313–318
3. Nagai N, Frank RM (1975) Transfert du Ca^{45} par Autoradiographie en Microscopie Electronique au Cours de L'Amelogenese. Calcif Tissue Res 19:211–221
4. Eisenmann DR, Ashrafi S, Neiman A (1979) Calcium transport and the secretory ameloblast. Anat Rec 193:403–422
5. Boyde A, Reith EJ (1977) Qualitative electron probe analysis of secretory ameloblasts and odontoblasts in the rat incisor. Histochem 50:347–354
6. Reith EJ, Boyde A (1978) Histochemical and electron probe analysis of secretory ameloblasts of developing rat molar teeth. Histochemistry 55:17–26
7. Engel M (1981) Microprobe analysis of calcifying matrices and formative cells in developing mouse molars. Histochemistry 72:443–452
8. Neiman A, Eisenmann DR (1975) The effect of strontium, cobalt and fluoride on rat incisor enamel formation. Anat Rec 183:303–322
9. Eisenmann DR, Ashrafi SH, Zaki AE (1982) Multi-method analysis of calcium localization in the secretory ameloblast. J Dent Res 61:1555–1561
10. Walton RE, Eisenmann DR (1974) Ultrastructural examination of various stages of amelogenesis following parenteral fluoride administration. Arch Oral Biol 19:171–182
11. Hall TA (1971) Microprobe assay of chemical elements. In: Oster G (ed) Physical techniques in biological research optical techniques, Vol. 1A, 2nd ed., Academic Press, New York, pp 157–275
12. Russ JC (1976a) Processing of energy dispersive x-ray spectra. EDAX Editor 6:4–39
13. Russ JC (1976b) An improved model to calculate pure element intensities in bulk samples. EDAX Editor 6:42–45
14. Boyde A, Reith EJ (1976) Scanning electron microscopy of the lateral cell surfaces of rat incisor ameloblasts. J Anat 122:603–610
15. Skobe Z (1980) Scanning electron microscopy of the mouse incisor enamel organ in transition between secretory and maturation stages of amelogenesis. Arch Oral Biol 25:395–401
16. Bawden JW, Wennberg A (1977) In vitro study of cellular influence on Ca^{45} uptake in developing rat enamel. J Dent Res 56:313–319
17. Kallenbach E (1980) Fate of horseradish peroxidase in the secretion zone of the rat incisor enamel organ. Tissue Cell 12:491–501
18. Sasaki T, Higashi S, Tachikawa T, Yoshiki S (1982) Formation of tight junctions in differentiating and secretory ameloblasts of rat molar tooth germs. Arch Oral Biol 27:1059–1068
19. Mulryan BJ, Neuman MW, Neuman WF, Toribara TY (1964) Equilibration between tissue calcium and injected radiocalcium in the rat. Am J Physiol 207:947–952
20. Borle AB (1967) Membrane transfer of calcium. Clin Orthop Rel Res 52:267–291
21. Crenshaw MA, Takano Y (1982) Mechanisms by which the enamel organ controls calcium entry into developing enamel. J Dent Res 61:1574–1579
22. Reith EJ (1983) A model for transcellular transport of calcium based on membrane fluidity and movement of calcium carriers within the more fluid microdomains of the plasma membrane. Calcif Tissue Int 35:129–134
23. Irving J (1973) Theories of mineralization of bone. Clin Orthop Rel Res 97:225–236
24. Gelpke C, Eisenmann DR (1980) Effects of cobalt on calcium transport in the secretory ameloblast as visualized by PPA. J Dent Res 59(A):811
25. Nikiforuk G, Fraser D (1979) Etiology of enamel hypoplasia and interglobular dentin: the roles of hypocalcemia and hypophosphatemia. Metab Bone Dis Rel Res 2:17–23